Enhanced Performance of N-Polar AlGaN-Based Ultraviolet Light-Emitting Diodes With Lattice-Matched AlInGaN Insertion in n-AlGaN Layer

Hongchang Tao, Shengrui Xu, Yanrong Cao, Huake Su, Yuan Gao, Yachao Zhang, Jincheng Zhang, *Member, IEEE*, and Yue Hao, *Senior Member, IEEE*

***Abstract*—AlGaN-based ultraviolet-A light-emitting diodes (UVA LEDs) inevitably suffer from current crowding effects at high injection levels due to their lateral device structure, resulting in non-uniform light emission and device overheating. In N-polar UV LEDs, the problem is further exacerbated by increased hole injection efficiency, leading to current crowding and aggravated hole leakage, which limits the device performance. An n-AlGaN/AlInGaN/AlGaN structure is adopted in this study, through modulation of the Al and In compositions in the AlInGaN quaternary alloy, lattice matching and greater bandgap of AlInGaN to AlGaN template is designed. The numerical results prove that the n-AlGaN/AlInGaN/AlGaN structure can promote current spreading and thus mitigate hole leakage, resulting in the significantly enhanced performance of N-polar UVA LEDs. Furthermore, the use of lattice-matched AlInGaN layers in practical epitaxy is feasible, which can avoid the defect introduction resulting from the lattice mismatch.**

***Index Terms*—AlInGaN, lattice-matching, UV LEDs.**

I. Introduction

AlGaN-based ultraviolet-A light-emitting diodes (UVA LEDs) have numerous application prospects, such as UV curing under room temperature in industry, lithography, gas sensing, and fast prototype construction [1]. In contrast to the conventional low or medium-pressure mercury lamps, AlGaN-based UVA LEDs offer advantages, including portable device size, energy conservation, and environmental friendliness [2], [3]. Consequently, AlGaN-based UVA LEDs have attracted considerable attention in recent years and are expected to replace mercury lamps as a new generation of UV light sources. Nevertheless, AlGaN-based UVA LEDs still confront the problems of low efficiency and low output power, which hinder the process to replace mercury lamps [4].

Various approaches have been proposed to promote the efficiency of AlGaN-based UVA LEDs. Improving the crystal quality of the AlGaN-based UVA structure is an important measure to improve internal quantum efficiency [1]. On the other hand, the high activation energy of the p-GaN acceptor, severe electron leakage, and high hole injection potential barrier lead to low hole injection efficiency. Therefore, some studies also focused on efficient p-type doping and energy band modulation [5], [6], [7], [8], [9], [10], [11], [12]. N-polar LEDs naturally exhibit a higher electron-blocking ability and hole injection efficiency than Ga-polar counterparts, which is promising for achieving high-efficiency UV light sources and has been intensively investigated recently [13], [14], [15], [16]. In addition, for a typical lateral UVA LEDs structure, p-type and n-type contact electrodes are placed on the same side, thus introducing a lateral current injection configuration that induces non-uniform current distribution at the edge of the n-side, i.e., the current crowding effect. The current crowding effect becomes prominent due to the imbalance of n- and p-type conductivity in AlGaN-based UV LEDs, leading to inhomogeneous light emission and significant efficiency degradation at high injection current induced by local Joule heating effects [17], [18]. Doping modulation of n-type or p-type regions has been proposed to achieve uniform current distribution by introducing a potential barrier [17], [19], [20]. A current blocking layer and electrode pattern design were also proposed to alleviate the current crowding effect [21], [22], [23]. However, the current crowding effect is aggravated by the inherent challenges posed by N-polar nitride materials. The high background carrier concentration makes p-type doping more challenging and leads to a more severe current crowding effect [24]. Moreover, the potential barrier for holes from the p-type region into the quantum well is relatively low in N-polar AlGaN-based UV LEDs. While this can enhance the efficiency of hole injection, it also contributes to the holes leakage through the active region to the n-type region before they are uniformly distributed. The hole leakage, in turn, leads to a reduction in the recombination rates of carriers in the quantum well.

To address the issues of current crowding and exacerbated holes leakage in N-polar AlGaN-based UV LEDs resulting from their low p-type conductivity and low hole injection barrier, a larger bandgap layer inserted into the n-type AlGaN region is

Manuscript received 23 May 2023; accepted 26 May 2023. Date of publication 30 May 2023; date of current version 7 June 2023. This work was supported in part by the National Key R&D Program of China under Grant 2022YFB3604400, in part by the National Science Basic Research Program of Shaanxi under Grant 2023-JC-JQ-56, in part by the National Natural Science Foundation of China under Grants 62074120, 62134006, and 62234013, in part by the Fundamental Research Funds for the Central Universities under Grant JB211108, and in part by the State Key Laboratory on Integrated Optoelectronics under Grant IOSKL2018KF10. *(Corresponding authors: Shengrui Xu; Yanrong Cao.)*

Hongchang Tao, Shengrui Xu, Huake Su, Yuan Gao, Yachao Zhang, Jincheng Zhang, and Yue Hao are with the State key Discipline Laboratory of Wide Bandgap Semiconductor Technology, School of Microelectronics, Xidian University, Xi'an 710071, China (e-mail: shengruixidian@126.com).

Yanrong Cao is with the School of Mechanical and Electrical Engineering, Xidian University, Xi'an 710071, China (e-mail: yrcao@mail.xidian.edu.cn).

Digital Object Identifier 10.1109/JPHOT.2023.3281342

feasible. This helps to balance the conductivity of the n- and p-regions and mitigate hole leakage, resulting in a more even current distribution and improved performance for N-polar UV LEDs. However, the $Al_xGa_{1-x}N$ insertion layer with a high aluminum fraction inevitably introduces the lattice mismatch with the AlGaN template, resulting in a degradation of crystal quality. Since the Al and In fraction in the $Al_xIn_yGa_{1-x-y}N$ quaternary can be independently tuned, a larger bandgap can be achieved while maintaining lattice matching with the AlGaN template. Therefore, a lattice-matched $Al_xIn_yGa_{1-x-y}N$ insertion layer in the n-type region can avoid crystal quality degradation while achieving current spreading, which is highly advantageous for N-polar UV LEDs.

In this study, we conducted numerical simulations to investigate the optical performance of N-polar AlGaN-based UVA LEDs (~365 nm) with a lattice-matched $Al_xIn_yGa_{1-x-y}N$ layer inserted into the n-AlGaN region. By sandwiching a thin n-$Al_xIn_yGa_{1-x-y}N$ layer within the n-AlGaN layer to form an n-AlGaN/n-$Al_xIn_yGa_{1-x-y}N$/n-AlGaN structure. The distributions of carrier concentrations, radiative recombination rates, and the energy band of both UV LEDs are simulated. Compared to the original structure with bulk n-AlGaN region, the insertion of the lattice-matched $Al_xIn_yGa_{1-x-y}N$ layer allowed for better current spreading and higher carrier recombination efficiency. Simulation results show that the wall-plug efficiency (WPE) of the UV LED with the n-AlGaN/n-$Al_xIn_yGa_{1-x-y}N$/n-AlGaN structure is higher than that of the original UV LED. Therefore, the simulation results suggest that the adoption of lattice-matched n-$Al_xIn_yGa_{1-x-y}N$ as a current spreading layer holds promising potential for mitigating the current crowding effect and the aggravated hole leakage issue in N-polar AlGaN-based UV LEDs.

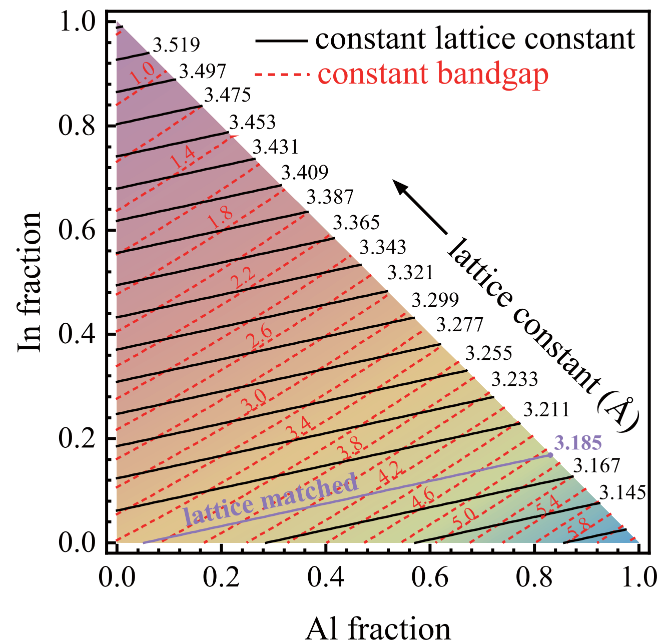

Fig. 1. Contours of constant lattice constant (black solid lines) and constant bandgap (red dashed lines) in $Al_xIn_yGa_{1-x-y}N$ layers as a function of the In and Al mole fractions.

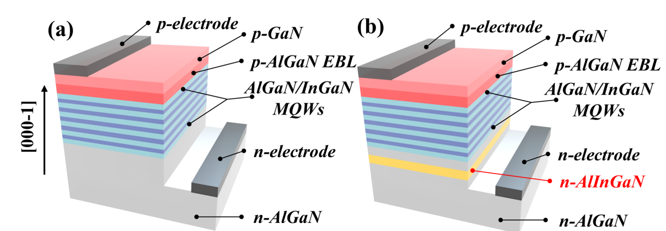

Fig. 2. Schematic diagrams of (a) structure A and (b) structure B.

II. Device Structures and Model

Firstly, as shown in Fig. 1, we present the bandgap and lattice constant of $Al_xIn_yGa_{1-x-y}N$ for different Al and In mole fractions. The calculation of $Al_xIn_yGa_{1-x-y}N$ material parameters including lattice constant and bandgap are adopted according to Ref. [25]. The range of compositions that match the lattice constant of the $Al_{0.05}Ga_{0.95}N$ template is indicated in Fig. 1. Considering selecting appropriate Al and In fraction to ensure lattice matching while achieving a larger bandgap compared to $Al_{0.05}Ga_{0.95}N$ template, an Al composition of 0.14 and an In composition of 0.02 were adopted.

As depicted in Fig. 2, we designed two structures of N-polar AlGaN-based UV LEDs to study the effect of n-$Al_{0.14}In_{0.02}Ga_{0.84}N$ insertion layer. One of them has a lattice-matched $Al_{0.14}In_{0.02}Ga_{0.84}N$ layer inserted in the n-type layer, and the other is a reference structure for comparison. Both structures are based on c-plane sapphire substrates with the growth direction of [000 1]. The structure, from bottom to top, consists of a 3-μm-thick n-type region ([Si] $= 3 \times 10^{18}$ cm^{-3}), a 5-cycle $Al_{0.1}Ga_{0.9}N/In_{0.02}Ga_{0.98}N$ multi-quantum wells (MQWs) active region with thicknesses of 10 nm and 3 nm, respectively. A 20-nm-thick p-$Al_{0.25}Ga_{0.75}N$ ([Mg] $= 5 \times 10^{18}$ cm^{-3}) electron blocking layer (EBL) to suppress electron leakage, and a 100-nm-thick p-GaN ([Mg] $= 1 \times 10^{19}$ cm^{-3}) hole supply layer. As depicted in Fig. 2(a), the reference LED structure, i.e., Structure A, its n-type region is composed solely of n-$Al_{0.05}Ga_{0.95}N$ ([Si] $= 3 \times 10^{18}$ cm^{-3}). While for Structure B (shown in Fig. 2(b)), the n-type region comprises 2.925-μm-thick $Al_{0.05}Ga_{0.95}N$ / 25-nm-thick $Al_{0.14}In_{0.02}Ga_{0.81}N$ /50-nm-thick $Al_{0.05}Ga_{0.95}N$, and the Si doping concentration is the same as Structure A. In the simulation, the size of the device dimension is 300 μm $\times$ 300 μm.

The numerical calculations were performed by the commercial packaged software Advanced Physical Model of Semiconductor Devices (APSYS) [26]. APSYS solves Poisson's equation, current continuity equation, and photon rate equation. In APSYS, the 6×6 k·p band theory including stress effects together with the self-consistent computational model of quantum well is used. The band offset ratio is assumed to be 0.5 for the III-nitride systems. The Shockley-Read-Hall recombination lifetime, the Auger coefficient, and the radiative recombination coefficient are set as 50 ns, 1×10^{-30} cm^6/s, and 2×10^{-11} cm^3/s, respectively. In addition, due to the screening effect resulting from the dislocations of III-nitride materials, a 40% theoretical

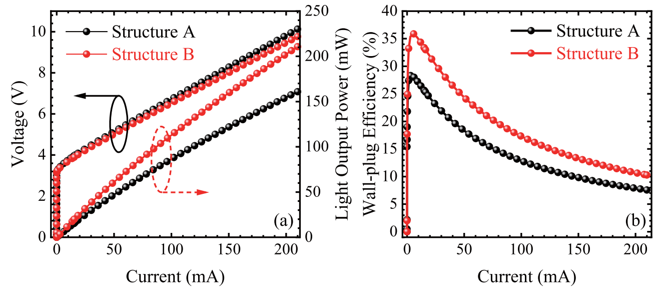

Fig. 3. Calculated (a) current-voltage (I-V) characteristics and light output power curves, and (b) wall-plug efficiency versus injection current for structure A and structure B.

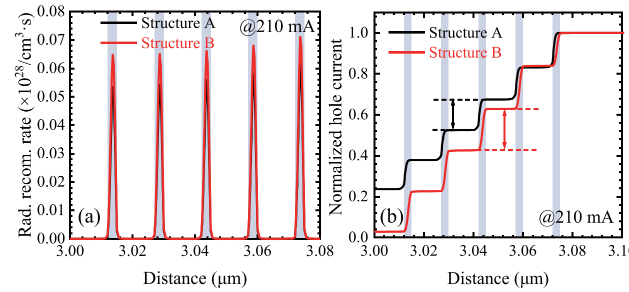

Fig. 5. (a) Radiative recombination rate in the active region and (b) normalized hole current across the MQWs active region of Structures A and B at the injection current of 210 mA.

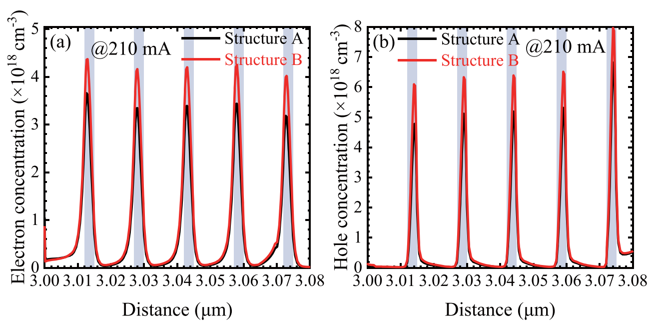

Fig. 4. Simulated (a) electron concentration and (b) hole concentration in the MQWs of structure A and B at the injection current of 210 mA.

polarization value is adopted in the simulation. Other material parameters used in this work can be found elsewhere [25].

III. Results and Discussions

We initially calculated the electrical characteristic and light output power curves of the Structures A and B to analyze the influence of the $Al_{0.14}In_{0.02}Ga_{0.84}N$ interlayer on the LED performance. As shown in Fig. 3, Structure B exhibits a lower forward voltage at the same current value compared to Structure A, and the forward voltage of structure B is reduced from 10.1 V to 9.7 V at 210 mA. The light output power of structure B is increased from 160.9 mW to 210.7 mW, which is boosted approximately by 30% through the $Al_{0.14}In_{0.02}Ga_{0.84}N$ insertion layer. As a result, Structure B exhibits higher WPE than that of Structure A.

To further explain the reason for the performance improvement of Structure B, analysis was conducted on the hole and electron concentrations in the MQWs active region. Fig. 4 shows the distribution of electron and hole concentrations in the quantum well under an injection current of 210 mA. It is evident that the electron and hole concentrations in the quantum well of Structure B are significantly promoted. The promoted carrier concentration is consistent with the results of Structure B, which exhibits higher light output power. Clearly, the insertion of the $Al_{0.14}In_{0.02}Ga_{0.84}N$ layer into the n-$Al_{0.05}Ga_{0.95}N$ region has a significant impact on the performance of the LEDs. It is reasonable to speculate that the larger bandgap induced by the $Al_{0.14}In_{0.02}Ga_{0.84}N$ layer enables the carrier redistribution. Moreover, it also effectively increases the hole concentration in the quantum wells.

To gain further insight into the impact of $Al_{0.14}In_{0.02}Ga_{0.84}N$ layer insertion on carrier transport, simulations of the hole current and radiative recombination rate at the injection current of 210 mA were conducted and presented in Fig. 5. Notably, the radiative recombination rate in the quantum well of Structure B was found to be significantly higher than that of Structure A, which is consistent with the higher carrier concentration Structure B. The higher electron and hole concentrations in Structure B led to a higher radiative recombination rate and a corresponding promotion in the light output power. Furthermore, Fig. 5(b) also shows that the normalized hole current of Structure B across the active region was significantly lower compared to that of Structure A, indicating a notable suppression of hole leakage current after $Al_{0.14}In_{0.02}Ga_{0.84}N$ layer insertion. The mitigated hole leakage is demonstrated for Structure B with $Al_{0.14}In_{0.02}Ga_{0.84}N$ insertion layer. As shown in Fig. 5(b), the normalized hole current is presented and the shadow area is the position of quantum wells. From left to right, the sequential representation in Fig. 5(b) corresponds to the MQWs active region and the p-type region. As illustrated in Fig 5(b), Structure B exhibits a nearly negligible normalized hole current value after passing through the first quantum barrier (The leftmost quantum well in Fig 5(b)), indicating minimal hole leakage into the n-type region. However, the transport direction of electrons is from the n-type region to the p-type region, opposite to the transport direction of holes. Therefore, the holes that do not participate in the recombination process within the quantum wells will leak into the n-type region, where they recombine with electrons before being injected into the active region. As a result, the leaked holes reduce the electron concentration injected into the MQWs as described in Ref. [27], leading to the higher electron concentration shown in Fig. 4(a). It is reasonable to speculate that the larger bandgap induced by the $Al_{0.14}In_{0.02}Ga_{0.84}N$ layer enables the carrier redistribution since the much-reduced hole leakage of Structure B compared with Structure A. Moreover, the decrease in hole current after crossing each quantum well was significantly larger in Structure B than in Structure A, suggesting that a higher concentration of holes within the quantum well participated in recombination rather than moving to the n-type regions, which might recombine with the electrons in the n-type regions, resulting in the decreased

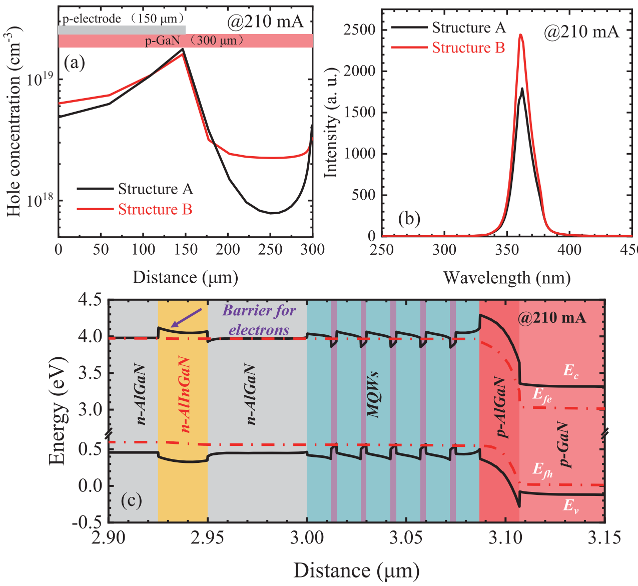

Fig. 6. (a) Simulated horizontal hole distribution in the last quantum well, (b) electroluminescence spectra of Structures A and B. (c) Energy band profile of structure B. The above results were all acquired at the injection current of 210 mA.

electron concentration injection into the active region. These findings suggest that the insertion of the $Al_{0.14}In_{0.02}Ga_{0.84}N$ layer can significantly improve the carrier transport properties of the device, thus leading to the enhanced performance as shown in Fig. 1. At last, we calculated and presented the lateral hole concentration distribution in the last quantum well at an injection current of 210 mA.

As shown in Fig. 6(a), horizontal hole distribution reveals the accumulation of high hole concentrations near the p-type electrode for both structures, which is attributed to the weakened conductivity of the p-type region compared with Structure A. However, for Structure B with the insertion of the $Al_{0.14}In_{0.02}Ga_{0.84}N$ layer, a more uniform and promotion of hole concentration distribution is realized. Fig. 6(b) provides the simulated electroluminescence (EL) spectra at 210 mA for both structures with peak wavelength of ∼365 nm, it is also noted that the peak EL intensity is greatly enhanced of Structure B compared with Structure A. Moreover, the band diagram of Structure B at 210 mA was calculated, and the results demonstrate that the insertion of the $Al_{0.14}In_{0.02}Ga_{0.84}N$ layer introduced electron potential barrier in the n-type region. The induced electron barrier thereby balanced the conductivity between the n-type and p-type regions of Structure B. As shown in Fig. 6(c), the electron potential barrier induced by the insertion layer is obvious, which would weaken the electron conductivity of the n-type region compared with that of Structure A. Since the current in a UV LED structure comprises both vertical and horizontal components, the ratio of vertical to horizontal current serves as an indicator of current crowding. A higher ratio indicates more severe current crowding, which signifies poor hole distribution in the region not covered by the p-electrode. According to Guo et al., an increased vertical resistance across the LED structure leads to a reduced ratio of vertical to horizontal current, indicating a mitigated current crowding effect [28]. Therefore, as depicted in Fig. 6(c), the electron barrier induced by the $Al_{0.14}In_{0.02}Ga_{0.84}N$ insertion layer enhances the lateral current in the p-type region. This enhancement promotes the lateral movement of holes, resulting in a more uniform hole distribution and improved current spreading, as demonstrated in Fig 6(a). The improved lateral current leads to a higher and more uniform hole distribution in the quantum well of Structure B compared to Structure A. Consequently, higher hole concentration and radiative recombination rates are achieved, as depicted in Figs. 4(a) and 5(a). The increased holes participated in the recombination in the quantum wells rather than leaking into the n-type region, which results in that fewer electrons can combine with the leaked holes before injection into the active region. The combined enhancements from both current spreading and reduction of holes leakage consequently result in a remarkable enhancement in the performance of the N-polar ultraviolet LED.

IV. Conclusion

In conclusion, we conducted a comprehensive analysis of the influence of incorporating a lattice-matched $Al_{0.14}In_{0.02}$-$Ga_{0.84}N$ insertion layer on the performance of N-polar ultraviolet LED devices. Simulation results revealed that the lattice-matched $Al_{0.14}In_{0.02}Ga_{0.84}N$ insertion layer effectively mitigates the current crowding effect and suppresses hole leakage. Consequently, there is an increase in the carrier concentrations, and an increase of 30% in the light output power. Moreover, the improved current spreading in turn led to a lower forward voltage, ultimately leading to higher WPE. It is reasonably believed that the lattice-matched $Al_xIn_yGa_{1-x-y}N$ insertion layer presents an effective method and offers numerous advantages in the growth of practical LED structures. With the appropriate Al and In fractions utilized, the AlInGaN current spreading can be extended to LEDs with different emission wavelength. The findings in this work provide a new method to achieve high-efficiency III-nitride LEDs. The proposed structure is feasible in the practical UV LEDs fabrication and avoid additional growth difficulty brought from the lattice-mismatching.

References

[1] M. Kneissl, T.-Y. Seong, J. Han, and H. Amano, “The emergence and prospects of deep-ultraviolet light-emitting diode technologies,” *Nature Photon.*, vol. 13, no. 4, pp. 233–244, Apr. 2019, doi: 10.1038/s41566-019-0359-9.

[2] M. Kneissl et al., “Advances in group III-nitride-based deep UV light-emitting diode technology,” *Semicond. Sci. Technol.*, vol. 26, no. 1, Jan. 2011, Art. no. 014036, doi: 10.1088/0268-1242/26/1/014036.

[3] Z. J. Ren et al., “Band engineering of III-nitride-based deep-ultraviolet light-emitting diodes: A review,” *J. Phys. D-Appl. Phys.*, vol. 53, no. 7, Feb. 2020, Art. no. 073002, doi: 10.1088/1361-6463/ab4d7b.

[4] A. Khan, K. Balakrishnan, and T. Katona, “Ultraviolet light-emitting diodes based on group three nitrides,” *Nature Photon.*, vol. 2, no. 2, pp. 77–84, Feb. 2008, doi: 10.1038/nphoton.2007.293.

[5] J. Simon, V. Protasenko, C. Lian, H. Xing, and D. Jena, “Polarization-induced hole doping in wide-band-gap uniaxial semiconductor heterostructures,” *Science*, vol. 327, no. 5961, pp. 60–64, Jan. 2010, doi: 10.1126/science.1183226.

[6] R. Chaudhuri, S. J. Bader, Z. Chen, D. A. Muller, H. G. Xing, and D. Jena, “A polarization-induced 2D hole gas in undoped gallium nitride quantum wells,” *Science*, vol. 365, no. 6460, pp. 1454–1457, Sep. 2019, doi: 10.1126/science.aau8623.

[7] H. Yu et al., “Enhanced performance of an AlGaN-based deep-ultraviolet LED having graded quantum well structure,” *IEEE Photon. J.*, vol. 11, no. 4, Aug. 2019, Art. no. 8201006, doi: 10.1109/JPHOT.2019.2922280.

[8] K. Kojima, K. Furusawa, Y. Yamazaki, H. Miyake, K. Hiramatsu, and S. F. Chichibu, “A design strategy for achieving more than 90% of the overlap integral of electron and hole wavefunctions in high-AlN-mole-fraction AlxGa1-xN multiple quantum wells,” *Appl. Phys. Exp.*, vol. 10, no. 1, Jan. 2017, Art. no. 015802, doi: 10.7567/APEX.10.015802.

[9] J. Lang et al., “High performance of AlGaN deep-ultraviolet light emitting diodes due to improved vertical carrier transport by delta-accelerating quantum barriers,” *Appl. Phys. Lett.*, vol. 114, no. 17, Apr. 2019, Art. no. 172105, doi: 10.1063/1.5093160.

[10] Z.-H. Zhang et al., “Hole transport manipulation to improve the hole injection for deep ultraviolet light-emitting diodes,” *Amer. Chem. Soc. Photon.*, vol. 4, no. 7, pp. 1846–1850, Jul. 2017, doi: 10.1021/acsphotonics.7b00443.

[11] C. Chu et al., “On the origin of enhanced hole injection for AlGaN-based deep ultraviolet light-emitting diodes with AlN insertion layer in p-electron blocking layer,” *Opt. Exp.*, vol. 27, no. 12, pp. A620–A628, Jun. 2019, doi: 10.1364/OE.27.00A620.

[12] N. Maeda, M. Jo, and H. Hirayama, “Improving the light-extraction efficiency of AlGaN DUV-LEDs by using a superlattice hole spreading layer and an Al reflector,” *Phys. Status Solidi A-Appl. Mater.*, vol. 215, no. 8, Apr. 2018, Art. no. 1700436, doi: 10.1002/pssa.201700436.

[13] H. Tao, S. Xu, X. Fan, J. Zhang, and Y. Hao, “Greatly enhanced wall-plug efficiency of N-polar AlGaN-based deep ultraviolet light-emitting diodes,” *IEEE Photon. J.*, vol. 13, no. 3, Jun. 2021, Art. no. 8200311, doi: 10.1109/JPHOT.2021.3084752.

[14] H. Tao, S. Xu, J. Zhang, P. Li, Z. Lin, and Y. Hao, “Numerical investigation on the enhanced performance of N-polar AlGaN-based ultraviolet light-emitting diodes with superlattice p-type doping,” *IEEE Trans. Electron Devices*, vol. 66, no. 1, pp. 478–484, Jan. 2019, doi: 10.1109/TED.2018.2878727.

[15] S. Xiao et al., “Performance evaluation of tunnel junction-based N-polar AlGaN deep-ultraviolet light-emitting diodes,” *Opt. Lett.*, vol. 47, no. 16, pp. 4187–4190, Aug. 2022, doi: 10.1364/OL.467685.

[16] Y. Zhao et al., “Performance enhancement of an N-polar nitride deep-ultraviolet light-emitting diode with compositionally graded p-AlGaN,” *Opt. Lett.*, vol. 47, no. 2, pp. 385–388, Jan. 2022, doi: 10.1364/OL.449099.

[17] H. Su et al., “Improving the current spreading by Fe doping in n-GaN layer for GaN-based ultraviolet light-emitting diodes,” *IEEE Electron Device Lett.*, vol. 42, no. 9, pp. 1346–1349, Sep. 2021, doi: 10.1109/LED.2021.3100545.

[18] E. Jung and H. Kim, “Rapid optical degradation of GaN-based light-emitting diodes by a current-crowding-induced self-accelerating thermal process,” *IEEE Trans. Electron Devices*, vol. 61, no. 3, pp. 825–830, Mar. 2014, doi: 10.1109/TED.2013.2297340.

[19] Y. Chen, J. Che, C. Chu, H. Shao, Y. Zhang, and Z.-H. Zhang, “Balanced resistivity in n-AlGaN layer to increase the current uniformity for AlGaN-based DUV LEDs,” *IEEE Photon. Technol. Lett.*, vol. 34, no. 20, pp. 1065–1068, Oct. 2022, doi: 10.1109/LPT.2022.3200460.

[20] R. Peng et al., “Green light-emitting diodes with improved efficiency by an in situ C-doping GaN current spreading layer,” *Opt. Lett.*, vol. 47, no. 16, pp. 4139–4142, Aug. 2022, doi: 10.1364/OL.468800.

[21] S. Zhou et al., “High-efficiency GaN-based LED with patterned SiO2 current blocking layer deposited on patterned ITO,” *Opt. Laser Technol.*, vol. 109, pp. 627–632, Jan. 2019, doi: 10.1016/j.optlastec.2018.08.049.

[22] S. Zhang et al., “Enhanced wall-plug efficiency in AlGaN-based deep-ultraviolet LED via a novel honeycomb hole-shaped structure,” *IEEE Trans. Electron Devices*, vol. 66, no. 7, pp. 2997–3002, Jul. 2019, doi: 10.1109/TED.2019.2913962.

[23] G. D. Hao, M. Taniguchi, N. Tamari, and S. Inoue, “Current crowding and self-heating effects in AlGaN-based flip-chip deep-ultraviolet light-emitting diodes,” *J. Phys. D-Appl. Phys.*, vol. 51, no. 3, Jan. 2018, Art. no. 035103, doi: 10.1088/1361-6463/aa9e0e.

[24] N. A. Fichtenbaum, T. E. Mates, S. Keller, S. P. DenBaars, and U. K. Mishra, “Impurity incorporation in heteroepitaxial N-face and Ga-face GaN films grown by metalorganic chemical vapor deposition,” *J. Cryst. Growth*, vol. 310, no. 6, pp. 1124–1131, Mar. 2008, doi: 10.1016/j.jcrysgro.2007.12.051.

[25] I. Vurgaftman and J. R. Meyer, “Band parameters for nitrogen-containing semiconductors,” *J. Appl. Phys.*, vol. 94, no. 6, pp. 3675–3696, Sep. 2003, doi: 10.1063/1.1600519.

[26] “APSYS (2016 version),” Crosslight Software, Inc., Burnaby, Canada. [Online]. Available: http://www.crosslight.com

[27] Y.-H. Shih et al., “Design of hole-blocking and electron-blocking layers in AlxGa1-xN-based UV light-emitting diodes,” *IEEE Trans. Electron Devices*, vol. 63, no. 3, pp. 1141–1147, Mar. 2016, doi: 10.1109/TED.2016.2520998.

[28] X. Guo and E. F. Schubert, “Current crowding in GaN/InGaN light emitting diodes on insulating substrates,” *J. Appl. Phys.*, vol. 90, no. 8, pp. 4191–4195, Oct. 2001, doi: 10.1063/1.1403665.